JCAMECH

Experimental measurement of heat transfer coefficient and mass of deposited CaSO₄ in subcooled flow boiling condition

A. Vosough [a], M.R. Assari [b,], S.M. Peyghambarzadeh [c,*]*

[a] Department of Mechanical Engineering, Dezful Branch, Islamic Azad University, Dezful, Iran
[b] Jundi-Shapur University of Technology, Dezful, Iran
[c] Department of Chemical Engineering, Mahshahr Branch, Islamic Azad University, Mahshahr, Iran

ARTICLE INFO

ABSTRACT

Fouling is a common, fundamental and costly problem in heat transfer systems, which reduces thermal efficiency of equipment, increases the energy loss and causes strong damage to the heat transfer equipment in various industries. The main causes of fouling on the heat transfer surfaces are salts with inverse temperature-solubility in the fluid which calcium sulfate is one of the most important of them. In this paper, the effect of calcium sulfate fouling on the heat transfer coefficient in subcooled flow boiling was investigated. The fouling mass of calcium sulfate on the heat transfer surface was also calculated. In the experiments carried out in this study, flow rate (2.5–11.5 l/min), solution concentration (1.75–2.2 g/l), bulk fluid temperature (55–75 ℃), and heat flux (8-95 kW/m²) were variables at the mentioned ranges. The results showed that the maximum deviation in the uncertainty analysis was related to the difference between the inlet and outlet temperature of the fluid, followed by the temperature difference between the wall temperature and the bulk fluid temperature. Also, the analysis of the experimental data revealed that increasing the salt concentration, the bulk temperature, and the heat flux of the solution, the mass of deposited calcium sulfate on the heat transfer surface increases with time, resulting in a decrease in the heat transfer coefficient. Careful analysis of the experimental data also showed that the solution concentration has more important role than the heat flux and the fluid bulk temperature in fouling formation.

1. Introduction

Fouling of heat exchange surfaces in convection heat transfer and subcooled flow boiling are a common problem in industrial processes. Fouling forms an unwanted layer over the heat exchange surface, which reduces the heat transfer coefficient, promotes corrosion, dissipates energy, and pollutes the environment. Calcium sulfate is a salt with inverse solubility (with respect to temperature) in water and causes the fouling of heat exchange equipment. Calcium sulfate scaling is a major concern in water desalination, geothermal electricity production, and petrochemical industries [1]. The production of phosphoric acid creates large amounts of calcium sulfate as a byproduct. Calcium sulfate is also an unwelcome deposit in the oil and gas industry, water cooling towers, hydrometallurgical processes, etc. The deposits can disrupt the equipment and the production process, which will be costly to remedy [2, 3]. Fouling results in a clogging of pipelines and equipment, blocking the movement of fluids and reducing the thermal efficiency of heat exchange surfaces. Therefore, numerous studies have been focused, and is underway, on calcium sulfate fouling mechanisms and methods for their prevention [4-9].

Lv et al. [10] performed an experimental study to survey the deposition formation of calcium carbonate solution on superhydrophobic surface with TiO₂ nanotube-array structure. They concluded that superhydrophobic nonporous coating has lower fouling resistance and better antifouling performance. Zhenhua et al. [11] performed an experimental study to analyze calcium carbonate scale formation on the heat transfer surface during forced convective heat transfer. In this work, an experimental system was prepared to measure the dynamic fouling resistance. Scale formation behavior was investigated under different operating conditions of flow velocity, salinity, hardness, bulk temperature, and surface temperature. They concluded that fouling formation rate, asymptotic resistance, and induction period increase with decreasing fluid velocity and increasing solution hardness, bulk temperature, and surface temperature. Al-Janabi et al. [12] experimentally investigated calcium sulfate fouling formation on the shot peened surfaces during forced convective heat transfer. Shot peened is a process performed on the surfaces to improve the surface characteristics against corrosion and

fatigue. In this process, abrasive material impinges the surface at the high velocity, causes the stimulation of residual stresses of lower layers of the surface and consequently, enhances the resistance property against corrosion and fatigue. They compared fouling formation on the shot peened and regular surfaces, and concluded that fouling induction period decreases up to 30%, and the overall heat transfer coefficient decreases up to 65% for shot peened surface. Furthermore, it was founded that deposited layer on the shot peened surfaces was harder, thicker, more adhesive, and less porous. In the previous studies, more attention has been paid to the heat transfer coefficient [10-16]. In the present study, in addition to investigating the heat transfer coefficient of calcium sulfate solution, the fouling mass developed on the heat transfer surface was investigated. After analyzing the uncertainty, the influence of important operating parameters (heat flux, solution concentration and bulk solution temperature) on the fouling mass under sub-cooled flow boiling condition was examined.

2. Experimental set up

As evident from Fig. 1, the setup was designed to allow the measurement of the heat transfer coefficient in annular space. For this purpose, a 316 stainless steel cylinder was placed vertically in a Plexiglas cylinder. Four E-type thermocouples with a 0–700 °C measurement range were embedded into the cylinder walls to measure the surface temperature. The liquid inlet and outlet temperatures were measured by two thermo-resistance (Pt-100Ω). The average of these two measured temperatures is determined as the local bulk temperature. A 15-cm-long and 12-cm-diameter heating element (bolt heater) capable of producing a heat flux of around 95 kW/m^2 was placed at the center of the steel cylinder. A centrifugal pump was used to set the fluid in motion. The pump outlet was equipped with a rotameter that measured the passing flow. A temperature-controller was used to adjust the heater temperature, prevent its overheating, and maintain the fluid temperature. Standard fittings were used for all cases, for which the pressure drop was assumed to be negligible. A 0–300 V autotransformer was used to control the central heating element in the main part of the setup and adjust the heat flux. The experimental methods and the boiling process are discussed in detail in the following section. The main parts of the setup with details (Annulus, thermocouples place, the main stainless-steel cylinder containing a bolt heater.) are shown in Fig.2. Table 1 lists the specifications for the components in the annular heating element.

3. Preparing Calcium solution with different concentrations

Aqueous CaSO$_4$ solutions of various concentrations were required for the crystalline scale formation experiments. Given the low solubility of calcium sulfate in distilled water, the conditions were improved by dissolving calcium nitrate tetrahydrate (Ca (NO$_3$)$_2$ 4H$_2$O) and sodium sulfate (Na$_2$SO$_4$) in the water to be able to achieve the required concentration. By dissolving the two chemicals in water and heating the solution and raising up to its required temperature, the following reaction takes place.

$$Ca(NO_3)_2.4H_2O + Na_2SO_4 \rightarrow CaSO_4 + 2NaNO_3 + 4H_2O \tag{1}$$
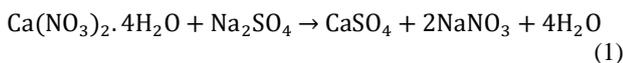
Figure 1. Image of experimental set up

Table 1. The specifications of the components in the annular heating element

Item	amount (mm)
Stainless steel cylinder diameter	20
Stainless steel cylinder length	300
Plexiglas diameter	40
Plexiglas length	400
Bolt heater diameter	120
Bolt heater length	150
Hydraulic diameter	20
Thermocouple length	7
Thermocouple diameter	1
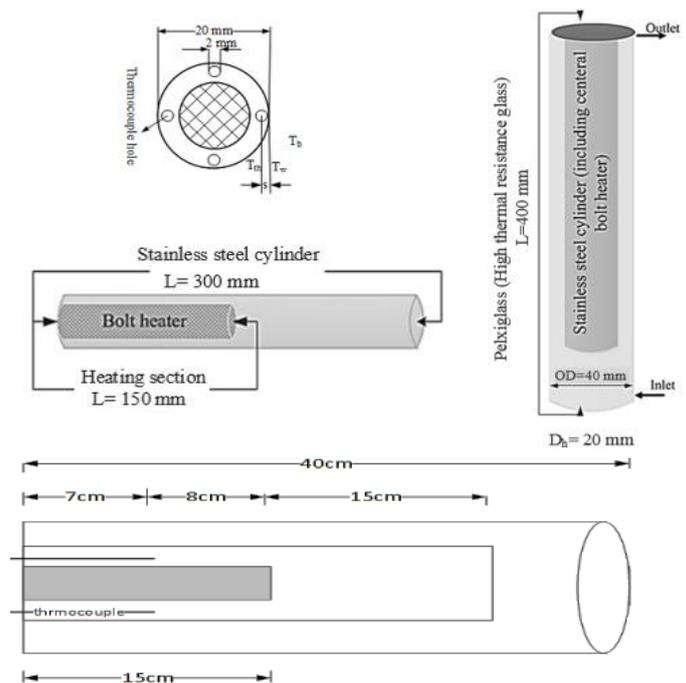
Figure 2. The main parts of the setup: The annulus and accessories (stainless steel cylinder, bolt heater, Plexiglas, thermocouples place)

The calcium sulfate concentration in the prepared solution is obtained by measuring the concentration of calcium ions by titration with Ethylenediaminetetraacetic acid (EDTA) [4, 17]. Table 2 summarizes the operating conditions.

Table 2. Operating conditions

Salt concentration	1.75-2.2 g/l
Fluid bulk temperature	55 – 75°C
Heat flux	8 – 95 kW/m²
Flow rate	2.5 – 11.5 l/min
Reynolds number	2700-11000
Operating system pressure	0.99 bar

4. Calibration of the Main Heating Element

Fig. 3 shows a schematic view of the position of the thermocouples inside the main heater. The thermocouple readings (T_{th}) are not the actual wall temperature (T_w) but higher. The temperature difference is a result of the thermal resistance of the heating element material present between the two points. The well-known Wilson plot technique [18] was used to calibrate the wall temperature. The well-known Wilson plot technique was used to calibrate the wall temperature [18]. The method will be explained briefly.
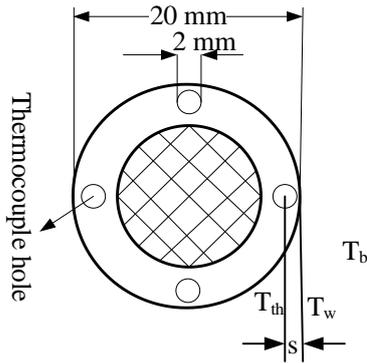
Figure 3. A schematic view of the placement of the thermocouples.

The heat transfer coefficient can be obtained based energy balance under steady-state conditions by Equation 2 [19].

$$h_{exp} = \frac{\dot{m}C_p(T_{out} - T_{in})}{A(T_w - T_b)} \qquad (2)$$

The actual surface temperature can be obtained by using Equation (3) according to Fourier's conduction law [20] .

$$T_w = T_{th} - q\left(\frac{s}{k}\right) \qquad (3)$$

By applying energy balance at steady state condition, the temperature differences can be related as Equation (4).

$$q = U(T_{th} - T_b) = h(T_w - T_b) = \frac{k}{s}(T_{th} - T_w) \qquad (4)$$

The above equation can be simplified as follows:

$$\frac{1}{U} = \frac{1}{h} + \frac{s}{k} \qquad (5)$$

If h can be calculated based on some system properties, such as velocity, the s/k ratio can be estimated using the above equation. So, the following relation is used [21].

$$h \propto f.Re \qquad (6)$$

For smooth tubes in turbulent flow, the friction factor is related to the Reynolds number (Re) through the Blasius correlation [22].

$$f \propto \frac{1}{Re^{0.25}} \qquad (7)$$

The combination of Eqs. (6) and (7) yields the following equation for the heat transfer coefficient.

$$h \propto Re^{0.75} \qquad (8)$$

Given that the fluid bulk temperature is constant in each experiment, the Re is proportional to the fluid velocity. The following relation is obtained considering the discussion and by considering all constants as β.

$$\frac{1}{U} = \frac{\beta}{V^{0.75}} + \frac{s}{k} \qquad (9)$$

Equation (9) shows that, by plotting 1/U against $1/V^{0.75}$ for each thermocouple, the intercept of the line is s/k. Using this method, the average s/k values for thermocouples were obtained for all heat fluxes of 5×10^{-4} m².K/W as shown in Fig 4. The fouling resistance is defined as follows:

$$R_f = \frac{1}{h_f} - \frac{1}{h_c} \qquad (10)$$

According to this definition, the amount of fouling mass per unit area on the heat transfer surface is calculated as follows:

$$m_f = \rho_f \lambda_f R_f \qquad (11)$$

If the density and conductivity of the fouling layer are constant m_f will be proportional to R_f. Table 3 shows the physical parameters used in this study.
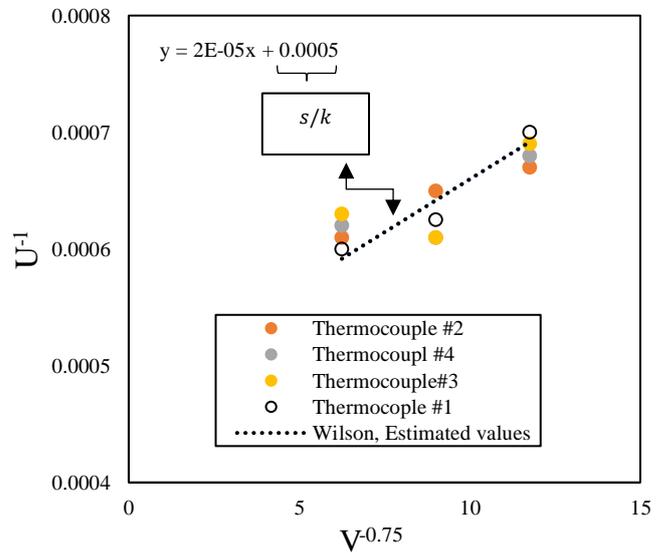
Figure4. Calculate the s/k coefficient

Table 3: Physical parameters used in this study [23].

Specification	amount
CaSO₄ fouling layer conductivity (k)	2160 kg/m³
CaSO₄ fouling layer density (ρ)	2.2 W/m°C

5. Uncertainty Analysis

In experimental studies, an uncertainty analysis is carried out by calculating the measurement error for different quantities. The maximum possible error in the measurable data can be calculated relying on this concept. In the present study, the uncertainty range of the heat transfer coefficient is the result of errors in the measurement of the volumetric flow rate, hydraulic diameter, and temperature differences. According to Muffat [24], the uncertainty of the heat transfer coefficient, was calculated at 20.21% using the following relations. Table 4 shows the accuracy of the measurement tools and the contribution of each parameter to the heat transfer coefficient uncertainty analysis (%).

$$h = f\{Q, A, (T_{out} - T_{in}), (T_w - T_b)\} \tag{12}$$

$$\left[\frac{\delta h}{h}\right]^2 = \left[1 \times \frac{\delta Q}{Q}\right]^2 + \left[(-1) \times \frac{\delta A}{A}\right]^2 + \left[1 \times \frac{\delta(T_{out}-T_{in})}{(T_{out}-T_{in})}\right]^2 + \left[(-1) \times \frac{\delta(T_w-T_b)}{(T_w-T_b)}\right]^2 \tag{13}$$

Table 4: the accuracy of the measurement tools and the percentage of contribution of each parameter to the heat transfer coefficient uncertainty analysis

parameters	Device measurement accuracy	contribution of each parameter to the heat transfer coefficient uncertainty analysis (%)
Length, Area	± 0.1mm	5.23
Volume flow rate	± 0.1 l/min	17.35
Temperature $(T_w - T_b)$	± 0.2 K	37.77
temperature $(T_{out} - T_{in})$	± 0.2 K	39.65

6. Results and discussion

Fig.5. illustrates the effect of heat flux on the heat transfer coefficient of distilled water. The data presented in this figure includes two regions: forced convection, and flow boiling heat transfer regions. Accurately identifying the two regions by increasing the heat flux is challenging, as it is contingent upon observing tiny bubbles on the heat transfer surface. Further, the transient region is affected by changes in the flow rate. But a closer look at the data reveals that the slope of the heat transfer coefficient increases sharply with increasing heat flux over the 20 -30 kW/m². That is due to the change in the heat transfer mechanism from forced convection to boiling, which is accompanied by tiny bubbles forming on the heat transfer surface. The bubbles can dissipate heat from the surface faster and suddenly increase the heat transfer coefficient. It was already proved in our previous research [16, 19, 25]. It must be emphasized that at lower heat fluxes, single-phase forced convection heat transfer is observed, following which, by increasing the heat flux, tiny bubbles start to form and rapidly vanish on the heat transfer surface as a result of their cold ambient. This phenomenon is called sub cooled flow boiling. As evident, most experimental data in this study has been done in the sub cooled flow boiling. In addition, it is also observable that in the single-phase forced-convection regime, the effect of heat flux on the heat transfer coefficient is negligible, while in the boiling region its effect is considerable.
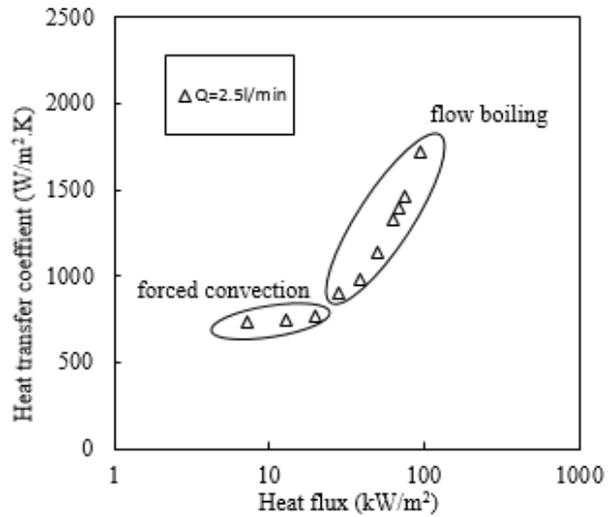
Figure 5. The effect of heat flux on the heat transfer coefficient of distilled water at Q = 2.5 l/min and Tb= 75 °C.

Fig. 6 shows the effect of heat flux on heat transfer coefficient at 1.75 g/l solution concentration and 11.5 l/ min volume flow rate. As shown in this figure, as the heat flux increases, the heat transfer coefficient initially increases and then decreases. Creation of primary crystal nucleation on the heat transfer surface, increases the surface roughness resulting in increasing in the active bubble generation sites. This phenomenon improves the heat transfer coefficient of $CaSO_4$ in the early stages of the experiments compared to the clean surface. This phenomenon has been observed in some previous studies [12, 26, 27]. The period when the heat transfer coefficient is higher than the start of the experiment is called the initial period or delay time. This time varies from a few minutes to several days depending on the test conditions. In this study, this time is estimated to be between 25-135 minutes. As the heat flux increases, the surface temperature raises, resulting in an increase in the evaporation of the micro-layers, which results in an increase in the saturation of the calcium sulfate solution. This causes more deposition at the surface of the heat transfer followed by a faster reduction of heat transfer coefficient. It is noteworthy that all the fluxes shown in this figure are in sub cooled flow boiling range and cause to generate bubbles on the surface of the heat transfer and evaporation of the microlayers.
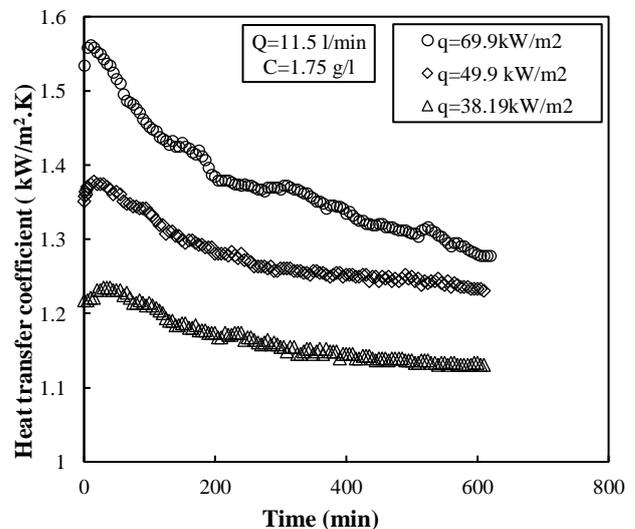
Figure 6. Influence of heat flux on heat transfer coefficient of $CaSO_4$ solution

In Fig. 7, the effect of heat flux on the fouling mass created on the heat transfer surface is discussed. As shown in this figure, as the heat flux increases, more deposition settles on the surface of the heat transfer and decreases its efficiency, which the reasons are explained in Fig. 5. To draw this figure, the fouling mass during the delay period is assumed zero because of limitation in the experimental method, whereas in reality this value is close to zero.
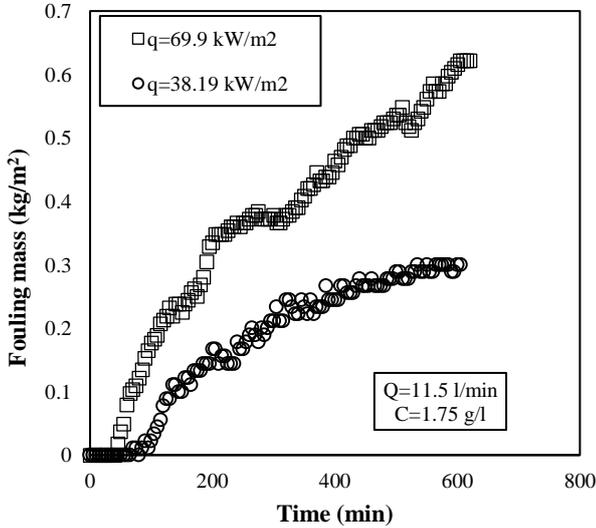
Figure 7. The effect of heat flux on the fouling mass on the heat transfer surface

Fig. 8 shows the effect of bulk temperature on the heat transfer coefficient of $CaSO_4$ solution at constant flow rate, solution concentration, and heat flux. Increasing the liquid bulk temperature, increases the surface temperature which leads to reduction of calcium sulfate solubility in the vicinity of the heat transfer surface. In other words, saturation concentration and consequently the degree of supersaturation are highly dependent on the bulk temperature. Both surface temperature and degree of supersaturation will increase the rate of deposition. In Fig.9, the effect of bulk temperature on the fouling mass of heat transfer surface with respect to constant conditions of other operating variables is discussed. As shown in this figure, as the bulk temperature increases, the fouling mass increases. Fig. 10 shows the effect of calcium sulfate concentration on the heat transfer coefficient. As can be seen, whenever the higher concentration of salt was used, more deterioration in the heat transfer coefficient was observed. Increasing the salt concentration causes the deposited layer on the heat transfer surface becomes thicker, and as a result, the surface temperature tends to rise. This effect leads to decrease the heat transfer coefficient in the solution with the higher salt concentration. Furthermore, it is clear that at t=0, when the heat transfer surface was clean, the solution with lower salt concentration showed greater heat transfer coefficient. Some other research confirmed the results of this study [7, 11, 25, 28]. Fig. 11. illustrates the effect of concentration with respect to constant conditions of other operating parameters (volume flow rate, bulk temperature and heat flux) on the heat transfer surface fouling mass. As shown in this figure, as the concentration increases, the amount of fouling mass on the surface of the heat transfer increases sharply, because the increase in concentration will increase the surface temperature and as a result the fouling mass. Further investigation of this figure shows that although the heat flux used
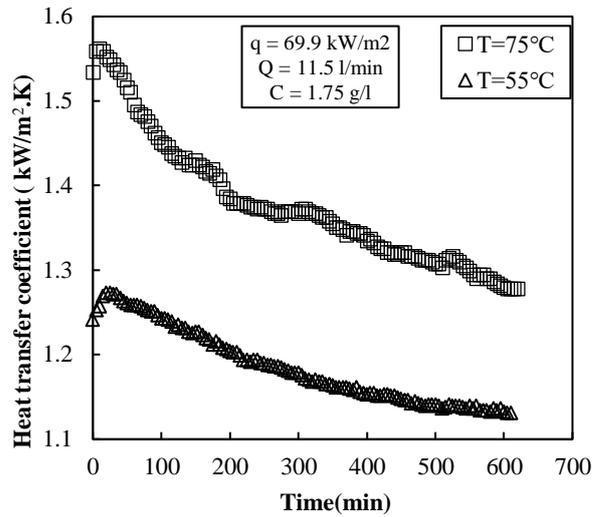
Figure 8. The effect of bulk solution temperature on the heat transfer coefficient
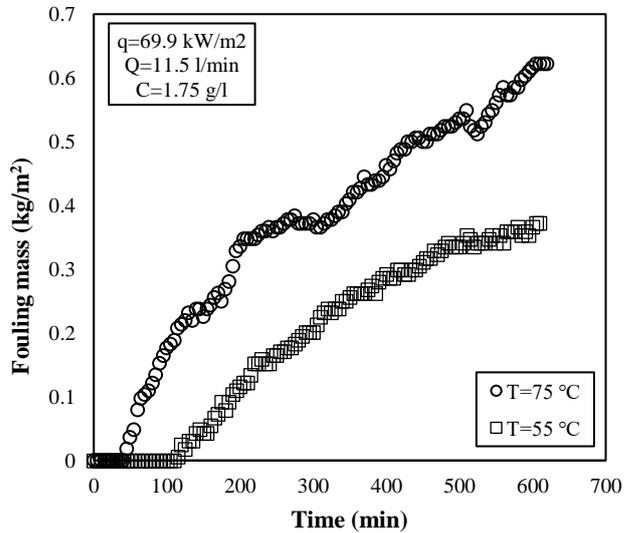
Figure 9. The effect of bulk solution temperature on the fouling mass
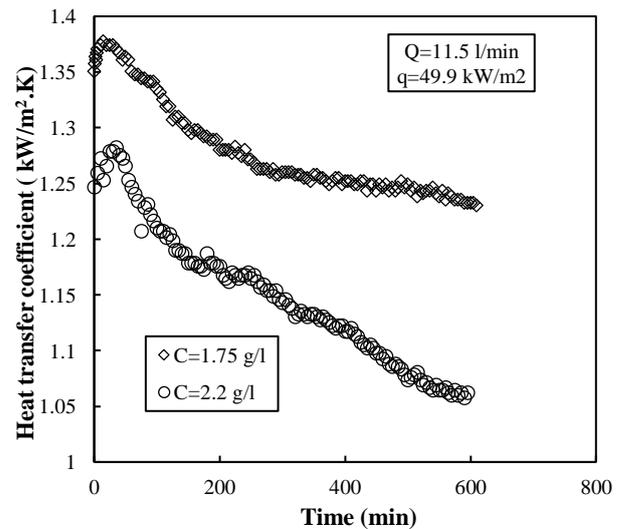
Figure 10. The effect of calcium sulfate solution concentration on the heat transfer coefficient

in this experiment is lower than other experiments (lower heat flux creates lower surface temperature) but higher fouling mass has

been created on heat transfer surface. This indicates that concentration has a stronger role in the formation of fouling than heat flux and bulk temperature.
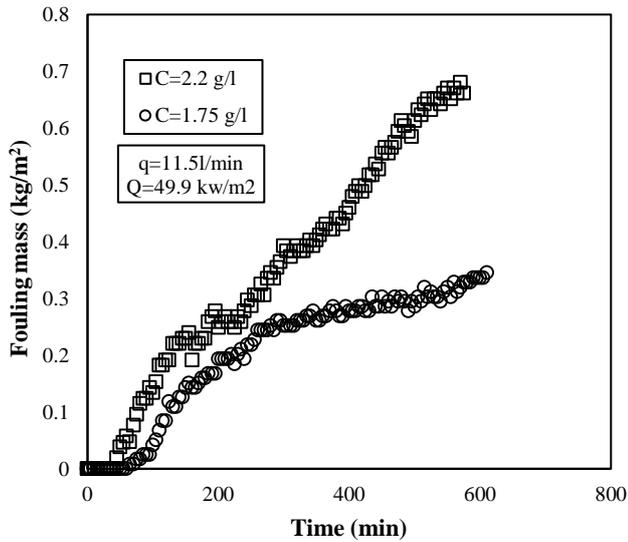
Figure 11. Effect of solution concentration according to constant conditions of other operating parameters (volume flow rate, bulk temperature and heat flux) on the fouling mass

7. Conclusion:

Fouling on the heat transfer surfaces decreases the heat transfer coefficient and consequently reduces the thermal efficiency. Calcium sulfate solution, which has inverse solubility over temperature, causes fouling on heat transfer surfaces. In this paper, after analyzing the uncertainty to ensure the accuracy of the experiments, the heat transfer coefficient and the mass of fouling layer were calculated and the effect of various parameters on them were investigated. The important results are as follows:

1. The maximum deviation in the uncertainty analysis is related to the difference between the inlet and outlet temperature of the fluid, followed by the temperature difference between the wall temperature and the bulk fluid temperature.

2. By increasing the heat flux under constant conditions of other operating variables (concentration, volume flow rate and bulk temperature), the heat transfer coefficient increases. At clean surface as the heat flux increases, the heat transfer coefficient increases and also the surface temperature increases, which causes more fouling to form. As the fouling is created, the heat transfer coefficient begins to decrease. Therefore, the system should be designed with the optimum heat flux.

3. Increasing the fluid bulk temperature increases the surface temperature, which causes increasing of the fouling mass on the heat transfer surface. As described above, the system should be designed at the optimal conditions so that both heat transfer coefficient and fouling mass are at their best condition.

4. Increasing the solution concentration reduces the heat transfer coefficient and increases the mass of the fouling. As the concentration increases, the temperature of the heat transfer surface increases over time and the fouling on the surface increases, which causes further reduction in the heat transfer coefficient.

5. Further investigation on of the experimental data showed that increase in salt concentration has a stronger role in the fouling formation than the heat flux and the bulk temperature. Increasing the heat flux and bulk temperature increases the initial heat transfer coefficient which is a positive point, and on the other hand increases the fouling mass which is a negative point, while increasing the solution concentration decreases the initial heat transfer coefficient and increases the fouling mass which both points are negative. Because of this two negative points, the effect of concentration is higher than other parameters in fouling formation.

8. Nomenclature

A	Heat transfer surface (m^2)
C	Concentration (g/l)
h	Heat transfer coefficient (W m^{-2} K^{-1})
f	Friction factor
L	Length (m)
$\dot{m}$	mass rate (kg s^{-1})
q	Heat flux (W m^{-2})
Q	Volume flow rate (m^3 s^{-1})
Re	Reynolds
R_f	fouling resistance (m^2. K W^{-1})
s	Distance between location of thermocouple and surface of heater (m)
T	Temperature (K)
U	Overall heat transfer coefficient (W m^{-2} K^{-1})
V	Velocity (m s^{-1})

Subscripts

b	Bulk
f	Fouling
l	Fluid
th	Thermocouple
w	wall

Greek symbols

ρ	density (kg m^{-3})
λ	Thermal conductivity (W/m^2. K)

9. References

[1] D. Aquilano, F. Otálora, L. Pastero, J. M. García-Ruiz, C. o. Materials, Three study cases of growth morphology in minerals: halite, calcite and gypsum, *Progress in Crystal Growth,* Vol. 62, No. 2, pp. 227-251, 2016.

[2] G. Van Rosmalen, P. Daudey, W. Marchee, An analysis of growth experiments of gypsum crystals in suspension, *Journal of Crystal Growth,* Vol. 52, pp. 801-811, 1981.

[3] J. Moghadasi, M. Jamialahmadi, H. Müller-Steinhagen, A. Sharif, Scale formation in oil reservoir and production equipment during water injection (Kinetics of CaSO4 and CaCO3 crystal growth and effect on formation damage), in *Proceeding of,* Society of Petroleum Engineers, pp.

[4] A. Helalizadeh, H. Müller-Steinhagen, M. Jamialahmadi, Mixed salt crystallisation fouling, *Chemical Engineering and Processing: Process Intensification,* Vol. 39, No. 1, pp. 29-43, 2000.

[5] A. Helalizadeh, H. Müller-Steinhagen, M. Jamialahmadi, Mathematical modelling of mixed salt precipitation during convective heat transfer and sub-cooled flow boiling, *Chemical Engineering Science,* Vol. 60, No. 18, pp. 5078-5088, 2005.

[6] S. N. Kazi, G. G. Duffy, X. D. Chen, Fouling and fouling mitigation on heated metal surfaces, *Desalination,* Vol. 288, pp. 126-134, 2012.

[7] M. H. Maddahi, M. S. Hatamipour, M. Jamialahmadi, Experimental study of calcium sulfate fouling in a heat exchanger during liquid-solid fluidized bed with cylindrical particles, *International Journal of Thermal Sciences,* Vol. 125, pp. 11-22, 2018.

[8] M. R. Malayeri, M. R. Jalalirad, Mitigation of crystallization fouling in a single heated tube using projectiles of different sizes and hardness, *Heat Transfer Engineering,* Vol. 35, No. 16-17, pp. 1418-1426, 2014.

[9] R. Steinhagen, H. Müller-Steinhagen, K. Maani, Problems and costs due to heat exchanger fouling in New Zealand industries, *Heat transfer engineering,* Vol. 14, No. 1, pp. 19-30, 1993.

[10] Y. Lv, M. Y. Liu, L. F. Hui, A. N. Pavlenko, A. S. Surtaev, V. S. Serdyukov, Heat Transfer and Fouling Rate at Boiling on Superhydrophobic Surface with TiO2 Nanotube-Array Structure, *Journal of Engineering Thermophysics,* Vol. 28, No. 2, pp. 163-176, 2019.

[11] Q. Zhenhua, C. Yongchang, M. A. Chongfang, Experimental study of fouling on heat transfer surface during forced convective heat transfer, *Chinese Journal of Chemical Engineering,* Vol. 16, No. 4, pp. 535-540, 2008.

[12] A. Al-Janabi, M. R. Malayeri, O. Badran, Performance of shot peened surfaces subject to crystallization fouling, *International Journal of Thermal Sciences,* Vol. 111, pp. 379-389, 2017.

[13] L.-C. Wang, S.-F. Li, L.-B. Wang, K. Cui, Q.-L. Zhang, H.-B. Liu, G. Li, Relationships between the characteristics of CaCO3 fouling and the flow velocity in smooth tube, *Experimental Thermal and Fluid Science,* Vol. 74, pp. 143-159, 2016.

[14] B. O. Hasan, E. A. Jwair, R. A. Craig, The effect of heat transfer enhancement on the crystallization fouling in a double pipe heat exchanger, *Experimental Thermal and Fluid Science,* Vol. 86, pp. 272-280, 2017.

[15] T. Hou, Y. Chen, Z. Wang, C. Ma, Experimental study of fouling process and antifouling effect in convective heat transfer under ultrasonic treatment, *Applied Thermal Engineering,* Vol. 140, pp. 671-678, 2018.

[16] A. Zangeneh, A. Vatani, Z. Fakhroeian, S. M. Peyghambarzadeh, Experimental study of forced convection and subcooled flow boiling heat transfer in a vertical annulus using different novel functionalized ZnO nanoparticles, *Applied Thermal Engineering,* Vol. 109, pp. 789-802, 2016.

[17] D. A. Skoog, D. A. West, F. J. Holler, Analytical Chemistry, 6th ed, *Sounders College Publishing* 1992.

[18] J. Fernández-Seara, F. J. Uhia, J. Sieres, Laboratory practices with the Wilson plot method, *Experimental Heat Transfer,* Vol. 20, No. 2, pp. 123-135, 2007.

[19] S. M. Peyghambarzadeh, A. Vatani, M. Jamialahmadi, Experimental study of micro-particle fouling under forced convective heat transfer, *Applied Thermal Engineering,* Vol. 29, No. 4, pp. 713-724, 2012.

[20] M. M. Sarafraz, S. M. Peyghambarzadeh, Experimental study on subcooled flow boiling heat transfer to water–diethylene glycol mixtures as a coolant inside a vertical annulus, *Experimental Thermal and Fluid Science,* Vol. 50, pp. 154-162, 2013.

[21] J. P. Holman, 2002, *Heat Transfer-Si Units-Sie*, Tata McGraw-Hill Education,

[22] B. S. Massey, 2006, *Mechanics of Fluids* Taylor & Francis, 8ed.

[23] S. M. Peyghambarzadeh, A. Vatani, M. Jamialahmadi, Application of asymptotic model for the prediction of fouling rate of calcium sulfate under subcooled flow boiling, *Applied Thermal Engineering,* Vol. 39, pp. 105-113, 2012.

[24] R. J. Moffat, Using uncertainty analysis in the planning of an experiment, *Journal of Fluids Engineering,* Vol. 107, No. 2, pp. 173-178, 1985.

[25] A. Vosough, S. M. Peyghambarzadeh, M. R. Assari, Influence of thermal shock on the mitigation of calcium sulfate crystallization fouling under subcooled flow boiling condition, *Applied Thermal Engineering*, pp. 114434, 2019.

[26] M. S. Abd-Elhady, M. R. Jalalirad, M. R. Malayeri, Influence of injected projectiles on the induction period of crystallization fouling, *Heat Transfer Engineering,* Vol. 35, No. 3, pp. 232-245, 2014.

[27] S. M. Peyghambarzadeh, N. Bahrami, Statistical analysis of calcium sulfate scaling under boiling heat transfer, *Applied Thermal Engineering,* Vol. 53, No. 1, pp. 108-113, 2013.

[28] S. H. Najibi, H. Müller-Steinhagen, M. Jamialahmadi, Calcium sulphate scale formation during subcooled flow boiling, *Chemical Engineering Science,* Vol. 52, No. 8, pp. 1265-1284, 1997.